Journal of Clinical Periodontology

Periodontally diseased tooth roots used for lateral alveolar ridge augmentation. A proof-of-concept study

Frank Schwarz, Vladimir Golubovic, Ilja Mihatovic and Jürgen Becker

Department of Oral Surgery, Universitätsklinikum Düsseldorf, Düsseldorf, Germany

Abstract

Objectives: To assess the efficacy of periodontally diseased tooth roots used as autografts for lateral ridge augmentation and two-stage early osseointegration of titanium implants.

Material and Methods: Ligature-induced periodontitis lesions were established at the maxillary premolars in $n = 8$ foxhounds. Extracted, scaled and root planed pre-molar roots (PM-P) as well as retromolar cortical autogenous bone (AB) blocks were used for horizontal ridge augmentation of mandibular chronic-type defects. At 12 weeks, titanium implants were inserted and left to heal for another 3 weeks. Histological analyses included crestal ridge width (CW), augmented area (AA) and bone-to-implant contact (BIC).

Results: Both PM-P and AB grafts were gradually organized and replaced by newly formed bone. Median CW (PM-P: 3.83 *versus* AB: 3.67 mm), AA (PM-P: 10.18 *versus* AB: 9.82 mm^2) and BIC (PM-P: 50.00% *versus* AB: 35.21%) values did not reach statistical significance between groups ($p > 0.05$, respectively). Histologically, PM-P grafts were not associated with any inflammatory cell infiltrates.

Conclusions: PM-P autografts may reveal a structural and biological potential to serve as an alternative autograft to AB.

It is well-known that the anorganic and organic composition of dentin closely resembles that of bone (Brudevold et al. 1960, Linde 1989).

In particular, its organic matrix is also dominated by collagen type I fibres and features non-collageneous proteins, such as phosphoproteins, osteocalcin, porteoglycans and glycoproteins (Becker et al. 1986; Linde 1989).

Accordingly, previous and recent experimental studies have focused on the usage of dentin as potential bone substitute in several defect models. Basically, it was reported that dentin used either as particulated or block autograft featured osteoconductive as well as osteoinductive properties and got involved in the bone remodelling process (Catanzaro-Guimaraes et al. 1986, Andersson et al. 2009, Andersson 2010, Bormann et al. 2012, Atiya et al. 2014, Qin et al. 2014). In a most recent experimental animal study performed in the canine, extracted tooth roots were also successfully used for localized horizontal alveolar ridge augmentation and a staged osseointegration of titanium implants. At 12 weeks, the application of differently conditioned

(i.e. endodontically treated and untreated healthy) extracted premolars resulted in a clinically important gain in ridge width, thus allowing the insertion of common two-piece titanium implants. Histologically, the transplanted roots were replaced by newly formed bone and equally supported the early phase of osseointegration. In particular, the median bone-to-implant contact (BIC) ranged from 36.96% to 50.79% and was comparable to those values (32.53% to 64.10%) noted for cortical autogenous bone blocks (Schwarz et al. 2016). Another potential clinical source to obtain autogenous dentin might also be periodontally diseased teeth that are scheduled for extraction. However, it is currently unknown to what extent an infected root surface may compromise bone formation at the defect site.

Therefore, this study aimed at histologically evaluating the efficacy of periodontally diseased tooth roots used as autografts for lateral ridge augmentation and two-stage early osseointegration of titanium implants in a canine model.

Material and Methods

Animals

A total of eight foxhounds (7 males, 1 female, age 22.9 ± 13.9 months, mean weight 40.3 ± 3.8 kg) with a fully erupted permanent dentition were included. During all experimental phases, the animals were fed once per day with soft-food diet and water *ad libitum*. The study protocol was approved by the appropriate local authority (Landesamt für Natur und Verbraucherschutz, Recklinghausen, Germany) and did conform to the ARRIVE Guidelines (Kilkenny et al. 2010). The experimental part of the study started after an adaption period of 4 weeks.

Anaesthesia protocol and experimental procedures

Each surgical intervention followed a standardized anaesthesia protocol (Schwarz et al. 2014, 2016). In particular, intramuscular sedation was accomplished with 0.01 mg/kg acepromazine (Vetranquil 1%; Ceva Tiergesundheit, Düsseldorf, Germany).

Subsequently, anaesthesia was initiated employing 21.5 mg/kg thiopental-sodium (Trapanal 2.5%; Altana GmbH, Konstanz, Germany) and inhalation anaesthesia performed by the use of oxygen and nitrous oxide and isoflurane. While anaesthetized, all animals received a constant rate infusion of lactated Ringer's solution to maintain hydration. Depth of anaesthesia was improved by intravenous injection of either 0.1 mg/kg piritramid (Dipidolor®; Janssen-Cilag GmbH, Neuss, Germany) or 0.1 mg/kg l-methadon. Intra-operative analgesia was accomplished by injecting 4.5 mg/kg carprofene (Rimadyl®; Pfitzer Pharma GmbH, Karlsruhe, Germany). For post-operative analgesia, 0.01 mg/kg buprenorphin (days 1–3, subcutaneous application twice per day) and 4.5 mg/kg carprofen (days 1–7, per os) were applied.

Experimental phases

This study was subdivided into three experimental phases.

Phase 1

In both upper quadrants, the maxillary premolars (PM2–PM4) were randomly allocated (RandList®; DatInf GmbH, Tübingen, Germany) to either a ligature induction of periodontitis lesions (PM-P) or were left untreated. In brief, at respective teeth of the PM-P group, the plaque control regimen was stopped and a double set of cotton ligatures was forced into a layered position directly apical of the gingival margin. In the same surgery, the mandibular pre-molars PM1–PM4 and molars M1–M2 were carefully separated and removed after the elevation in mucoperiosteal flaps. Subsequently, in each hemimandible, three standardized box-type defects (9 mm in height from the crestal bone, 6 mm in depth from the surface of the buccal bone and 10 mm in width mesio-distally, maintenance of the lingual bone plate) were prepared at a distance of 5 mm with a straight fissure carbide bur under copious irrigation using sterile 0.9% physiological saline. A primary wound closure was achieved by means of mattress sutures (Resorba®, Nürnberg, Germany).

The maxillary ligatures were removed after an active breakdown

period of 4–6 months, when approximately 30% of the initial bone support was lost. This was verified by bone sounding procedures using a periodontal probe (PCP 12; Hu-Friedy, Tuttlingen-Moehringen, Germany).

Phase 2

Both mandibular quadrants were randomly (RandList®) allocated to PM-P and PM-C groups. In each hemimandible, the available three defects were randomly (RandList®) augmented with $2 \times PM$ (i.e. PM-P or PM-C) and $1 \times AB$, thus resulting in a total of $2 \times PM-P$, $2 \times PM-C$ and $2 \times AB$ grafts per animal. Specimens of the PM-C group as well as the corresponding AB group were scheduled for biomechanical analyses (i.e. removal torque testing). These results will be presented elsewhere. Accordingly, the present analysis reports on the contra-lateral hemimandibles having received PM-P and AB grafts.

In the upper jaws, PM-P were carefully extracted after vertical tooth separation ($n = 3$ teeth) (Fig. 1a). Thereafter, the crown was horizontally decapitated at the cemento–enamel junction, and the exposed dental pulp was preserved. Each surface of the extracted roots was adequately debrided and planed [i.e. scaling and root planing (SRP)] using Gracey curets (Hu-Friedy Co., Chicago, Illinois, USA) (Fig. 1b). The absence of calculus was evaluated by tactile sensation with a periodontal probe (PCP12; Hu-Friedy Co.).

Subsequently, mucoperiosteal flaps were elevated in the lower jaws and all the granulation tissue was carefully removed from the chronic-type defects ($n = 24$ experimental sites) (Fig. 1c). Both roots of each PM-P were size adapted in a way that their coronal-apical extension matched at best the mesio-distal width of the respective defect site. Whenever possible, two roots were aligned parallel to the alveolar bone crest (upper root: epicrestal position; lower root: rotated by 180 degree to fit at best the closest caudal position) with their inter-proximal (i.e. mesial or distal) surfaces facing the defect wall (Schwarz et al. 2016) (Fig. 1d and Supplementary Fig. S1). To support ankylosis at these (downward)
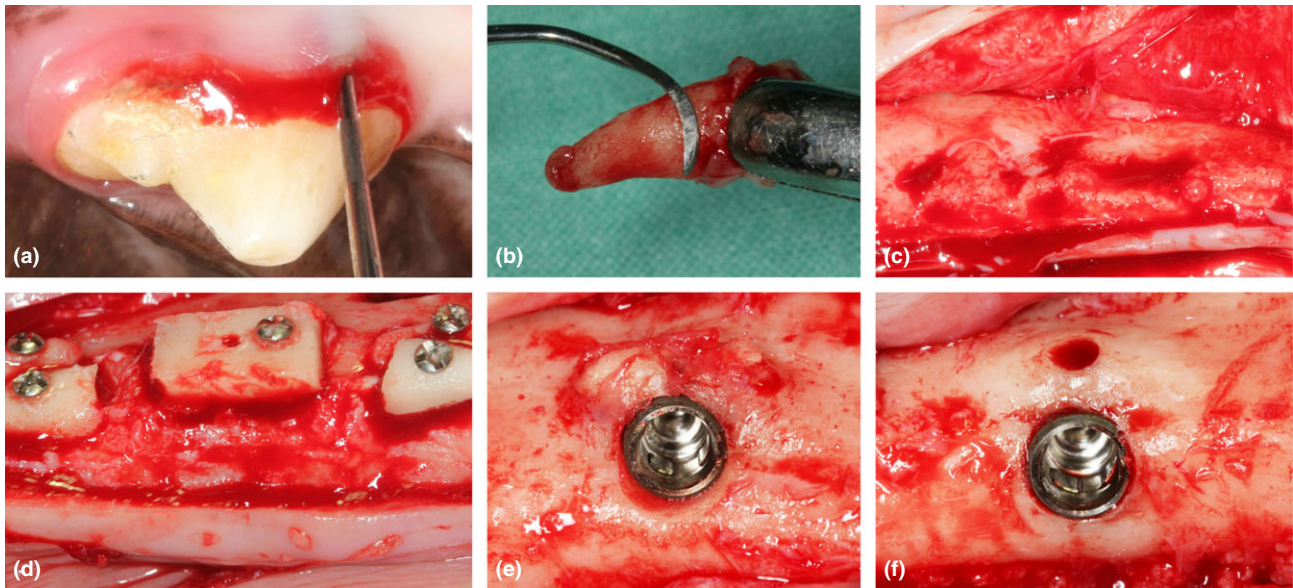
Fig. 1. (a) Established ligature-induced periodontitis lesion at maxillary pre-molar PM2. (b) Following crown decapitation, the extracted roots were adequately debrided and planed. (c) Clinical view of mandibular, chronic-type lateral alveolar ridge defects. (d) PM-P grafts were adapted in a way that one upper root was located in an epicrestal position. Whenever possible, a second root was rotated by 180 degree to fit at best the closest caudal position. To support ankylosis at root surface areas facing the defect wall (i.e. downward aspect), the layer of cementum was carefully removed until the underlying dentin was entirely exposed. In contrast, to reduce peripheral graft resorption, the cementum layer was preserved at the upward and lateral aspects of the transplanted roots. (e) After 12 weeks of submerged healing, two-piece titanium implants were inserted at the transition between the host bone and the grafted area (AB group). The experimental sites were submerged for another healing period of 3 weeks. (f) Similar to AB, PM-P grafts were also homogeneously organized by a newly formed hard tissue.

aspects of the roots (Andreasen 1980), the layer of cementum was carefully removed using a diamond bur under copious saline irrigation. At the upward and lateral aspects of the roots, the cementum was preserved. In each hemimandible, one cortical AB block exhibiting a surface area and thickness similar to the PM-P grafts was harvested from the retromolar area using a carbide bur and copious saline irrigation. PM-P and AB grafts were fixed with titanium osteosynthesis screws (P/5, 1.5×9 mm; Medicon, Tuttlingen, Germany) (Fig. 1d). The resulting horizontal width at each augmented site was measured using a calliper (i.e. from the most crestal aspect of the alveolar ridge to the most peripheral and coronal aspect of the graft). Coronally advanced mucoperiosteal flaps were fixed with mattress sutures (Resorba®) to ensure a tension-free submerged healing condition.

Phase 3

At 12 weeks, full thickness flaps were prepared and implant bed preparation was performed at the transition between the host bone and

the grafted area. Two-piece Bone Level® SLA® titanium implants (4.1×10 mm; Institut Straumann AG, Basel, Switzerland) were inserted with primary stability (i.e. lack of clinical implant mobility) in a way so that the implant shoulder (IS) at best coincided with the buccal aspect of the grafted area (Fig. 1e,f). Mucoperiosteal flaps were advanced, repositioned coronally and fixed with mattress sutures (Resorba®) in a way to ensure submerged healing for another 3 weeks.

Sample size calculation

Calculation of the sample size was based on a non-inferiority testing of PM-P to AB blocks (Schwarz et al. 2016). For the power analysis, a standard normal distribution was assumed. The probability of a Type I error was set at 0.05, whereas the probability of a Type II error was set at 0.20. Sigma was estimated based on the standard deviations observed in previous pre-clinical studies employing the same defect model (Schwarz et al. 2008, 2010). Defining ridge width as primary outcome variable, a clinically relevant

difference was arbitrarily set at 2 mm. To achieve 95% power, a sample size of eight animals was calculated (Power and Precision, Biostat, Englewood, USA).

Retrieval of specimens

At the end of phase 3, the animals were euthanized with an overdose of sodium pentobarbital 3%. The jaws were dissected and blocks containing the experimental specimens were obtained. All specimens were fixed in 10% neutral buffered formalin solution for 4–7 days.

Histological preparation

Histological preparation was performed according to a standardized procedure reported previously (Schwarz et al. 2011). In brief, the tissue biopsies were dehydrated using ascending grades of alcohol and xylene, infiltrated and embedded in methylmethacrylate (MMA) (Technovit 9100 NEU, Heraeus Kulzer, Wehrheim, Germany) for non-decalcified sectioning. Two sections approximately 300 μm in thickness were prepared from the most central

aspect of the implant in the vestibulo-oral direction using a diamond band saw (Exakt®; Apparatebau, Norderstedt, Germany) and ground to a final thickness of approximately 40 μm. All sections were stained with toluidine blue (TB) to evaluate new bone formation and to identify the histological landmarks (Schwarz et al. 2016). With this technique, old bone stains light blue, whereas newly formed bone stains dark blue because of its higher protein content (Schenk et al. 1984).

Histological analysis

Digital images (original magnification ×200) were taken from each section and evaluated using a software program (Cell D®; Soft Imaging System, Münster, Germany).

The following landmarks were identified in the stained sections at the vestibular aspect (Schwarz et al. 2016): IS, the bottom of the bone defect (BD) and the most central vertical axis (VA) of the implant. At or below the level of IS, the crestal width (CW) of the augmented alveolar ridge was measured as the horizontal linear distance from VA to the most peripheral and coronal aspect of the bone crest (BC) (mm). The new bone-to-implant contact (BIC) was measured from IS to BD, serving as 100%. In addition, the surface of the augmented area (AA) (mm^2) was measured from IS to BD (Fig. 2).

Statistical analysis

The statistical analysis was performed using a commercially available software program (SPSS Statistics 22.0; SPSS Inc., Chicago, IL, USA). Mean values and standard deviations among animals were calculated for each variable and group. The data rows were examined with the Kolmogorow–Smirnow test for normal distribution. Within-group comparisons (i.e. PM-P versus AB) defining the animal as statistical unit were accomplished using the unpaired *t*-test. The alpha error was set at 0.05.

Results

Clinical observations

The clinical width of the augmented area at phase 2 was 4.31 ± 0.66 in the PM-P and 4.1 ± 0.33 mm in the corresponding AB group, respectively. Health status, behaviour and feeding habits of each animal were uneventful during the course of the experimental phases.

A premature exposure of the augmented area was noted at 5 of 24 sites (i.e. AB = 2; PM-P = 3).

Clinically, the exposed grafts were not associated with any signs of wound infection, but separated from the host bone, thus preventing implant placement during phase 3. The remaining experimental sites were characterized by a persistence of the grafted volume and organization of PM-P and AB grafts by a newly formed hard tissue. A primary implant stability could not be obtained at four defects (i.e. AB = 2; PM-P = 2), thus resulting in a successful placement of $n = 15$ implants at respective sites (Fig. 1e,f).

Histomorphometrical analysis

The mean and median values of CW, AA and BIC in PM-P and AB groups are presented in Table 1.

In particular, median CW was 3.83 mm in the PM-P and 3.67 mm in the AB group. Median AA was 10.18 mm^2 in the PM-P and 9.82 mm^2 in the AB group. Median BIC was 50.00% in the PM-P and 35.21% in the AB group. The statistical analysis failed to reveal any significant differences in mean CW, AA and BIC values between PM-P and AB groups ($p > 0.05$; unpaired *t*-test), respectively (Table 1).

Histological description

Histological analysis revealed that PM-P grafts were gradually involved in the bone remodelling process. This was commonly characterized by the deposition of a parallel-fibred
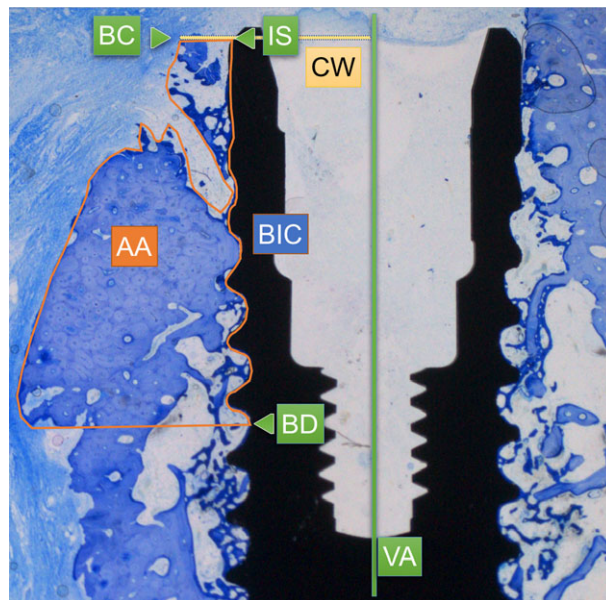

Fig. 2. Landmarks defined for the histomorphometrical analysis (specimen of the AB group, TB stain). AA: the augmented surface area (mm^2) was measured from IS to BD; BC: the most peripheral and coronal aspect of the bone crest at or below the level of IS; BD: the bottom of the bone defect; BIC: bone-to-implant contact (BIC) was measured from IS to BD; CW: crestal width of the alveolar ridge at the augmented site measured as the horizontal linear distance from VA to BC (mm); VA: the most central vertical axis of the implant; IS: implant shoulder.

Table 1. Histomorphometrical analysis (mean $\pm$ SD, median) of CW (mm), AA (mm^2) and BIC (%) values in PM-P and AB groups at the vestibular aspect ($n = 8$ animals)

Group	CW		AA		BIC	
PM-P	3.63 ± 0.84	3.83	11.01 ± 4.37	10.18	51.66 ± 24.07	50.00
AB	3.49 ± 0.59	3.67	8.07 ± 5.64	9.82	33.24 ± 26.53	35.21
p value*	0.55		0.69		0.89	

*Between-group comparisons (unpaired *t*-test): ns $p > 0.05$; respectively.

woven bone circumferentially along the external surface of the transplanted roots. Bone formation appeared to be originating from the adjacent alveolar bone and clearly demarcated the autografts at respective sites (Fig. 3).

In all specimens investigated, there were clear histological signs for a replacement resorption of PM-P. However, the extend of graft resorption varied considerably between and within animals, and even among the PM-P specimens in the same defect area. The majority of the experimental sites were characterized by the co-existence of PM-P grafts showing either initial to more advanced or even completed stages of replacement resorption (Fig. 3a–c). In particular, the initial stages were characterized by a peripheral resorption of the transplanted roots by macrophages. This was commonly accompanied by the concomitant deposition of a well-vascularized, connective tissue matrix exhibiting numerous spots of mineralization (Fig. 3d). At more advanced sites, the outer surface of the roots was homogeneously replaced by a parallel-fibred woven bone, which also extended restiformly, thus invading the dentinal matrix in various directions. The interface between the root fragments and the adjacent implant surface was homogeneously filled by a thin layer of woven bone, thus establishing an intimate BIC (Fig. 3e). At some sites, the transplanted roots were completely resorbed and substituted by a network of woven bone originating from the surrounding areas. Bone formation was obviously bridged by residual root fragments, which were occasionally noted in the most central aspects of AA at respective sites (Fig. 3c,f).

In none of the sites investigated, PM-P grafts were associated with the establishment of any inflammatory cell infiltrates.

Histological analysis also revealed signs for a replacement resorption of AB grafts. However, the ratio between graft resorption and new bone formation distinctly varied among the specimens investigated. In particular, at some sites, bone remodelling just comprised the most crestal compartment of the block graft, whereas AB was almost
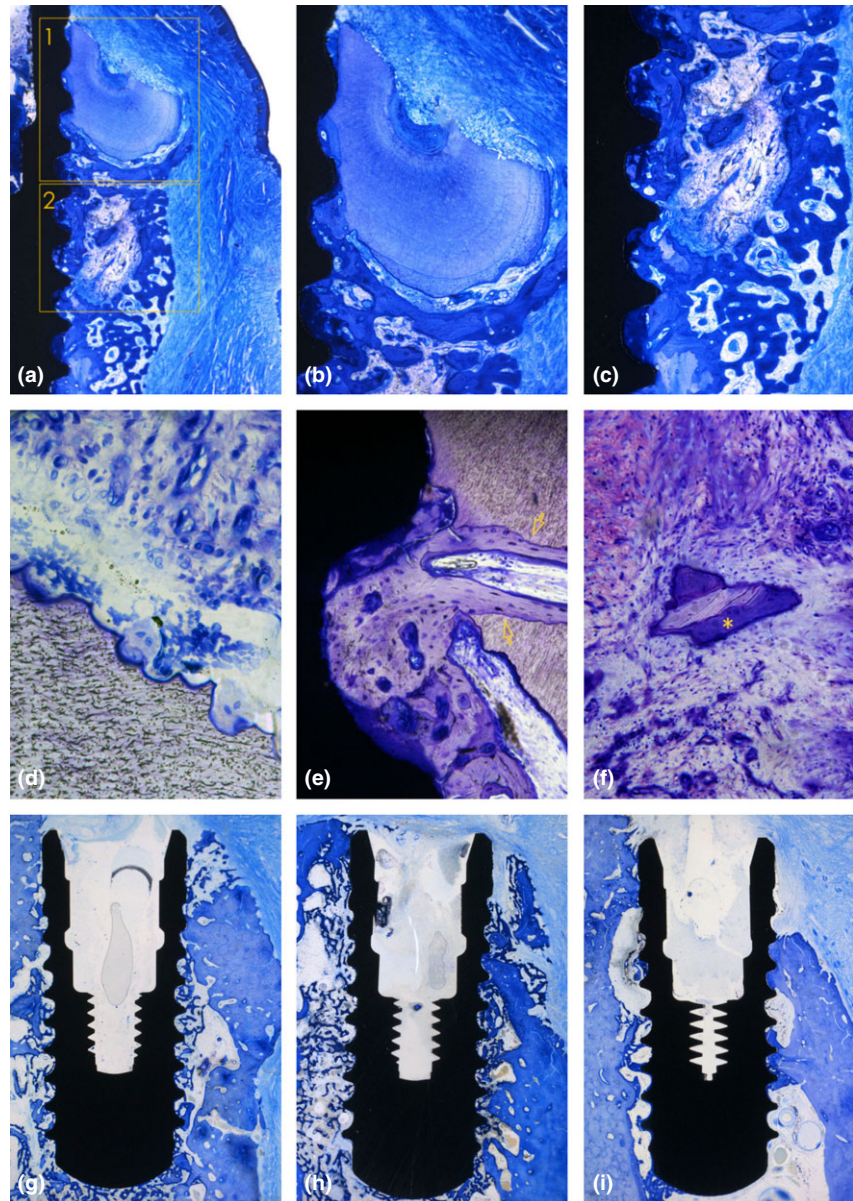

Fig. 3. Representative histological views of wound healing in PM-P and AB groups (TB stain). PM grafts were gradually involved in the bone remodelling process and replaced by a parallel-fibred woven bone. The extend of graft resorption commonly varied among PM-P specimens. (a) PM-P specimen showing signs for an initial (1.) and almost completed (2.) replacement resorption (original magnifications ×2.5). (b) Circumferential bone formation along the external surface of PM-P (higher magnification view ×4.5 of area 1. Depicted in Fig. 3a). (c) Complete resorption of PM-P and replacement by tiny trabeculae of woven bone (higher magnification view ×4.5 of area 2. Depicted in Fig. 3a). (d) Peripheral resorption of PM-P by macrophages and concomitant deposition of a mineralized connective tissue matrix (original magnifications ×40). (e) Interposition of woven bone (arrows) between PM-P grafts and the implant surface, thus establishing an intimate BIC (higher magnification view ×40). (f) Residues of PM-P bridged bone formation at the central aspect of AA (higher magnification view ×40 of Fig. 3c). (g) A replacement resorption was also noted for AB grafts (original magnifications ×1.5). (h) Specimen of the AB group showing a pronounced resorption of the transplanted matrix (higher magnification view ×1.5). (i) At some sites, the resorption rate of AB exceeded that of new bone formation (higher magnification view ×1.5).

unaltered within the central compartment of AA (Fig. 3g). However, at other sites, the bone remodelling process was more pronounced and resulted in a resorption of larger parts of AB without a concomitant

substitution of the matrix by newly formed bone (Fig. 3h,i).

Discussion

This proof-of-concept study aimed at assessing the influence of a ligature-induced periodontal infection on the structural and biological potential of extracted tooth roots to serve as alternative autografts to AB for horizontal alveolar ridge augmentation and two-stage early osseointegration of two-piece titanium implants in a standardized experimental animal model (Schwarz et al. 2008). Basically, it was observed that the clinical and histological outcomes of healing following application of PM-P grafts were comparable to those noted at the control sites investigated. In particular, both types of autografts (i.e. PM-P and AB) resulted in a clinically important gain in ridge width as well as similar median CW and AA values. Notably, median BIC measured at 3 weeks after implant placement was even elevated in the PM-P group (i.e. 50.00% *versus* 35.21%), however, this difference did not reach statistical significance over the AB group. Moreover, both PM-P and AB grafts were associated with comparable exposure rates, which mainly had to be attributed to this challenging experimental model (Rothamel et al. 2009, Schwarz et al. 2010).

When interpreting these results, it must be emphasized that a potential drawback of the study protocol was the lack of healthy roots serving as additional control group (PM-C). Even though these PM-C grafts were implemented in the contra-lateral hemimandibles, they were considered for biomechanical measurements (i.e. removal torque testing) at respective sites (Becker et al. 2016). However, since a most recent study employing the same defect model and experimental procedures reported on the histological analysis of PM-C grafts (Schwarz et al. 2016), this experimental set-up was modified to comply with the 3R principle and reduce the number of animals. When comparing the data of this analysis with those findings reported in the latter study, however, it might be suggested that the histological outcomes of healing did not seem to differ between PM-P and PM-C groups. In particular, for PM-C autografts, median CW, AA and BIC values were 2.70 mm, 7.55 mm^2, and 36.96%, respectively. In the corresponding AB group, these values amounted to 3.30 mm, 8.56 mm^2 and 64.10%, respectively. The differences between PM-C and AB grafts also failed to reach statistical significance (Schwarz et al. 2016).

These BIC values mainly reflect the early stage of osseointegration, and were also within the range of those data noted when SLA surfaced titanium implants were inserted at pristine bone sites. After a submerged healing period of 2 weeks in the lower jaws of the canine, respective BIC values ranged between 58.8% and 59.3% (Schwarz et al. 2007a,b).

All these data, taken together with the results of this study, seem to indicate that a meticulous SRP procedure appeared to be sufficient to restore the structural and biological potential of PM autografts that were exposed to a ligature-induced periodontal infection. In this context, one has to realize that a periodontal regeneration has also been shown on previously diseased root surfaces (Sculean et al. 2008, 2015), thus implying that SRP is a feasible measure to restore the biocompatibility of an infected layer of cementum. Moreover, it must be emphasized that the present surgical protocol considered a complete cementum removal and dentin exposure at the downward aspect of the roots to facilitate ankylosis at the defect site. The rational for this procedure was based on previous findings that damages to the periodontal ligament or root surface were more likely to result in ankylosis and subsequently a replacement resorption (Andreasen 1980). In contrast, to reduce a peripheral graft resorption, the cementum was preserved at the upward and lateral aspects of the roots.

However, when further evaluating the present histological analysis, it was obvious that a replacement resorption commonly happened at both inward (i.e. dentin) and outward (i.e. cementum) surface layers of PM-P grafts. This closely corroborates the histological outcomes noted following fixation of autogenous tooth grafts in the mandible of rabbits. In particular, the specimens were positioned with the dentin layer towards the defect and the enamel layer facing the mucosal compartment. At 6 months, the authors reported on a homogeneous and comparable replacement resorption at both outer and inner layers of the grafts (Qin et al. 2014).

Similar stages and histological features of a replacement resorption were also noted for PM-C specimens (Schwarz et al. 2016), thus suggesting that the dentin matrix of both PM-C and PM-P grafts was comparably integrated in the bone remodelling process. However, it was also noted that the transplanted roots in the PM-P group were more homogeneously replaced by newly formed bone than the AB grafts. Indeed, previous studies have indicated that cortical bone blocks are associated with an incomplete revascularization and a "creeping substitution process", which results in a composition of non-vital necrotic and newly formed vital bone (Burchardt & Enneking 1978, Burchardt 1983). Accordingly, the remodelling process associated with PM seems to be more similar to that reported for cancellous bone blocks, also undergoing a more rapid and complete replacement resorption (Burchardt & Enneking 1978, Burchardt 1983). In this context, however, one has to emphasize that the extend of PM-P resorption varied considerably among the sites and specimens investigated. Similar histological variations were also noted for PM-C as well as endodontically treated PM grafts (Schwarz et al. 2016). This might be explained by potential differences in the size and shape of the transplanted grafts, but also variations in the thickness of the cementum layer. Accordingly, future studies should further elaborate on the potential influence of the macro-and microanatomical characteristics of PM grafts on the process of replacement resorption.

Within the limitations of this proof-of-concept study, it was concluded that PM-P autografts may reveal a structural and biological potential to serve as an alternative autograft to AB.

References

Andersson, L. (2010) Dentin xenografts to experimental bone defects in rabbit tibia are ankylosed and undergo osseous replacement. *Dental Traumatology* **26**, 398–402.

Andersson, L., Ramzi, A. & Joseph, B. (2009) Studies on dentin grafts to bone defects in rabbit tibia and mandible; development of an experimental model. *Dental Traumatology* **25**, 78–83.

Andreasen, O. (1980) Analysis of pathogenesis and topography of replacement root resorption (ankylosis) after replantation of mature permanent incisors in monkeys. *Swedish Dental Journal* **4**, 231–240.

Atiya, B. K., Shanmuhasuntharam, P., Huat, S., Abdulrazzak, S. & Oon, H. (2014) Liquid nitrogen-treated autogenous dentin as bone substitute: an experimental study in a rabbit model. *International Journal of Oral and Maxillofacial Implants* **29**, 165–170.

Becker, J., Schuppan, D., Benzian, H., Bals, T., Hahn, E. G., Cantaluppi, C. & Reichart, P. (1986) Immunohistochemical distribution of collagens types IV, V, and VI and of pro-collagens types I and III in human alveolar bone and dentine. *Journal of Histochemistry and Cytochemistry* **34**, 1417–1429.

Becker, K., Drescher, D., Hönscheid, R., Golubovic, V., Mihatovic, I. & Schwarz, F. (2016) Biomechanical, micro-computed tomographic and immunohistochemical analysis of early osseous integration at titanium implants placed following lateral ridge augmentation using extracted tooth roots. *Clinical Oral Implants Research* doi: 10.1111/clr.12803. [Epub ahead of print].

Bormann, K. H., Suarez-Cunqueiro, M. M., Sinikovic, B., Kampmann, A., von See, C., Tavassol, F., Binger, T., Winkler, M., Gellrich, N. C. & Rücker, M. (2012) Dentin as a suitable bone substitute comparable to ss-TCP–an experimental study in mice. *Microvascular Research* **84**, 116–122.

Brudevold, F., Steadman, L. T. & Smith, F. A. (1960) Inorganic and organic components of tooth structure. *Annals of the New York Academy of Sciences* **85**, 110–132.

Burchardt, H. (1983) The biology of bone graft repair. *Clinical Orthopedics and Related Research* **58**, 28–42.

Burchardt, H. & Enneking, W. F. (1978) Transplantation of bone. *Surgical Clinics of North America* **58**, 403–427.

Catanzaro-Guimaraes, S. A., Catanzaro Guimaraes, B. P., Garcia, R. B. & Alle, N. (1986) Osteogenic potential of autogenic demineralized dentin implanted in bony defects in dogs. *International Journal of Oral and Maxillofacial Surgery* **15**, 160–169.

Kilkenny, C., Browne, W., Cuthill, I. C., Emerson, M., Altman, D. G. & NC3Rs Reporting Guidelines Working Group (2010) Animal research: reporting in vivo experiments: the ARRIVE guidelines. *British Journal of Pharmacology* **160**, 1577–1579.

Linde, A. (1989) Dentin matrix proteins: composition and possible functions in calcification. *Anatomical Record* **224**, 154–166.

Qin, X., Raj, R. M., Liao, X. F., Shi, W., Ma, B., Gong, S. Q., Chen, W. M. & Zhou, B. (2014) Using rigidly fixed autogenous tooth graft to repair bone defect: an animal model. *Dental Traumatology* **30**, 380–384.

Rothamel, D., Schwarz, F., Herten, M., Ferrari, D., Mischkowski, R. A., Sager, M. & Becker, J. (2009) Vertical ridge augmentation using xenogenous bone blocks: a histomorphometric study in dogs. *International Journal of Oral and Maxillofacial Implants* **24**, 243–250.

Schenk, R. K., Olah, A. J. & Herrmann, W. (1984) Preparation of calcified tissues for light microscopy. In: Dickson, G. R. (ed). *Methods of Calcified Tissue Preparation*, (pp. 1–56). Amsterdam: Elsevier.

Schwarz, F., Becker, K., Golubovic, V. & Mihatovic, I. (2016) Extracted tooth roots used for lateral alveolar ridge augmentation. A proof-of-concept study. *Journal of Clinical Periodontology* **43**, 345–353.

Schwarz, F., Ferrari, D., Balic, E., Buser, D., Becker, J. & Sager, M. (2010) Lateral ridge augmentation using equine- and bovine-derived cancellous bone blocks: a feasibility study in dogs. *Clinical Oral Implants Research* **21**, 904–912.

Schwarz, F., Ferrari, D., Herten, M., Mihatovic, I., Wieland, M., Sager, M. & Becker, J. (2007a) Effects of surface hydrophilicity and microtopography on early stages of soft and hard tissue integration at non-submerged titanium implants: an immunohistochemical study in dogs. *Journal of Periodontology* **78**, 2171–2184.

Schwarz, F., Herten, M., Sager, M., Wieland, M., Dard, M. & Becker, J. (2007b) Histological and immunohistochemical analysis of initial and early osseous integration at chemically modified and conventional SLA titanium implants: preliminary results of a pilot study in dogs. *Clinical Oral Implants Research* **18**, 481–488.

Schwarz, F., Mihatovic, I., Golubovic, V., Eick, S., Iglhaut, T. & Becker, J. (2014) Experimental peri-implant mucositis at different implant surfaces. *Journal of Clinical Periodontology* **41**, 513–520.

Schwarz, F., Rothamel, D., Herten, M., Ferrari, D., Sager, M. & Becker, J. (2008) Lateral ridge augmentation using particulated or block bone substitutes biocoated with rhGDF-5 and rhBMP-2: an immunohistochemical study in dogs. *Clinical Oral Implants Research* **19**, 642–652.

Schwarz, F., Sahm, N., Mihatovic, I., Golubovic, V. & Becker, J. (2011) Surgical therapy of advanced ligature-induced peri-implantitis defects: cone-beam computed tomographic and histological analysis. *Journal of Clinical Periodontology* **38**, 939–949.

Sculean, A., Nikolidakis, D., Nikou, G., Ivanovic, A., Chapple, I. L. & Stavropoulos, A. (2015) Biomaterials for promoting periodontal regeneration in human intrabony defects: a systematic review. *Periodontology 2000* **68**, 182–216.

Sculean, A., Nikolidakis, D. & Schwarz, F. (2008) Regeneration of periodontal tissues: combinations of barrier membranes and grafting materials - biological foundation and preclinical evidence: a systematic review. *Journal of Clinical Periodontology* **35**, 106–116.

Supporting Information

Additional Supporting Information may be found in the online version of this article:

Figure S1. Orientation and fixation of PM-P grafts to match the coronal-apical and mesio-distal extensions of respective defect sites.

Address:
Ilja Mihatovic
Department of Oral Surgery
Universitätsklinikum Düsseldorf
Westdeutsche Kieferklinik
D-40225 Düsseldorf, Germany
E-mail: Ilja.Mihatovic@med.uni-duesseldorf.de

Clinical Relevance

Scientific rationale for the study: Differently conditioned (i.e. endodontically treated and untreated) extracted tooth roots were successfully used for localized alveolar ridge augmentation and a staged osseointegration of titanium implants. Periodontally diseased teeth (PM-P) may also serve as potential clinical source to obtain autogenous dentin.

Principal findings: Following SRP, the application of PM-P was associated with a marked gain in horizontal ridge width. Histologically, the transplanted roots were gradually replaced by newly formed bone and supported the early osseointegration of titanium implants on a level equivalent to that noted for AB.

Practical implications: Following SRP, periodontally diseased roots were successfully used for localized alveolar ridge augmentation and a staged osseointegration of titanium implants.